Int. J. Heat Mass Transfer. Vol. 21, pp. 827–834

0017-9310/78/0701-0827 $02.00/0

FORECAST OF THE SURFACE STRUCTURE OF MOON, MARS, MERCURY AND VENUS BASED ON RADIO-ASTRONOMICAL OBSERVATIONS OF THEIR THERMAL CONDITIONS

G. N. DULNEV, YU. P. ZARICHNYAK and B. L. MURATOVA

Leningrad Institute of Precision Mechanics and Optics, U.S.S.R.

(*Received* 11 *March* 1976)

Abstract—The latest advances in the theory of heat transfer in heterogeneous systems, that is modelling of complex structures, make it possible, from the analysis of the precision radio-physical observations of thermal conditions on planets, to solve the inverse problem, which is determination of the soil texture of planets from their thermophysical properties.

The suggested method coupled with remote sensing of electro-physical and optical properties (dielectric constant and magnetic permeability, attenuation and polarization of radiation) allows the forecast of the soil structure of Earth's nearest neighbours in the solar system—the Moon, Mars, Mercury and Venus.

NOMENCLATURE

I_ν, spectral radiation intensity of the surface layer of the planet under study [W/m^3];
T, temperature [K];
y, surface layer depth [m];
τ, time;
q, density of heat flux from the planet interior [W/m^2];
σ, Stefan–Boltzmann constant [W/m^2 K^4];
R_l, R_{ir}, light and infrared albedo, respectively;
S_0, solar constant [W/m^2];
ϕ, ψ, longitude and latitude of the surface element considered;
Ω, lunation frequency;
$\gamma_{calc}, \gamma_{exp}$, calculated and measured values of the complex;
$\lambda, \lambda_k, \lambda_1, \lambda_g$, effective thermal conductivity surface layer, frame ("skeleton"), grains and gas in infinite space at atmospheric pressure and temperature T[W/mK];
λ_{r1}, radiative component of gas thermal conductivity in the gap between two grains [W/mK];
$\lambda_{r2}, \lambda_{m2}$, thermal conductivity in interconnecting pores due to molecular transfer and radiation [W/mK];
λ_r, λ_m, radiative and molecular thermal conductivity components in the pores of the second-order structure [W/mK];
m_2^0, m_2, total porosity of the system before and after deformation (consolidation);
m_{2k}^0, porosity of loosely strewed grains layer (unconsolidated bed);
m_{22}, porosity of the second-order structure;
κ, relative total deformation of structure during consolidation (condensing, sintering);
κ_k, relative deformation of frame ("skeleton") of granular system during consolidation;
N, coordination number equal to mean number of grains in contact with any particle;
c_s, specific heat of soil [J/kgK];
ρ, ρ_0, volume density of soil and rock (monolith) [kg/m^3];
$y_2 = r_2/r$, relative average radius of actual contact spot of deformed grains;
$y_3 = r_3/r$, relative average radius of grain cross section per unit contact;
$y_4 = r_4/r$, relative average radius of a circular pore per unit contact;
δ_1, δ_2, mean dimension of pores between frame grains, and of large pores of the second-order structure [m];
a, accommodation coefficient characterizing the extent of energy exchange at collision of gas molecules with soil particles;
Λ, mean gas free path length at atmospheric pressure and temperature T[m];
Pr, Prandtl number;
c_p/c_v, adiabatic index, ratio of isobaric and isochoric specific heats of gas in pores;
Φ, function allowing for variation of grain thermal resistance due to spreading of a heat flux entering the grain via the contact spot;
α, radiation attenuation constant due to

absorption and dissipation over the grain surface;
r, d, grain radius and diameter [m];
$\nu_i = \lambda_i/\lambda_j$, thermal conductivity ratio;
H, gas-filler pressure [N/m^2];
$c = \Delta/L$, (see Fig. 1c) space lattice (second-order structure) geometrical parameters ratio;
ε, emissivity.

INTRODUCTION

ONE OF the ways of securing information on the structure of planetary surfaces is the study of the unsteady temperature field of the surface layer of a planet by the use of radio astronomical methods. From the measured spectral radiation intensity, I_ν, of the planet in the wavelength range from 10×10^{-6} to 1.5 m, one may estimate its thermal radiation intensity over a span from 3 to 30 μm and, hence, the brightness temperature of the radiator [1, 2]. The thus measured temperatures are close to the average-volume temperature of a layer whose thickness (depth) is consistent with the wavelength at which the radiation intensity is measured in the r.f. band. Analysis of the radiation intensity at different frequences yields average-volume temperature of the surface layers of different thicknesses, and, thereby, the temperature distribution through this layer (from several centimetres to several metres). Such measurements can be taken both on the solar-irradiated (diurnal) and dark (nocturnal) surfaces of the planet, permitting one to get information on the nature of the planetary temperature field at different conditions of interplanetary orientation.

Finally, the knowledge of the temperature history in the vicinity of a terminator, which is a conventional boundary between the illuminated and dark areas of the planet throughout a lunation (change of lunar day and night) and during partial solar eclipses provides information on the unsteady temperature field of the planet surface.

Radiation receivers can be placed both on Earth (radio telescopes) and on spacecrafts which can approach the planet of interest. The radiation intensity is measured within a spherical angle of several angular minutes, the temperatures being averaged for planet surface areas of the diameters from several kilometers (space-based measurements) to hundred kilometers (Earth-based radio-telescopic observations).

The measurements of the temperature field in the surface layer of the planet are interpreted with the aid of the thermal semi-spatial model [1, 2]. The equation to describe the temperature variation $T(y, \tau)$ in the planet soil through the depth y and with time τ is of the form

$$\frac{\partial}{\partial y}\left[\lambda(y, T)\frac{\partial T}{\partial y}\right] = \rho(y)c_s(y, T)\frac{\partial T}{\partial \tau}. \qquad (1)$$

For a periodic thermal regime (lunation) the boundary conditions are as follows

$$\left(\lambda\frac{\partial T}{\partial y}\right)_{y=0} = \sigma(1 - R_{ir})T^4(0, \tau) + q - A$$

$$A = \begin{cases} S_0(1 - R_l)\cos\psi\cos(\Omega\tau - \phi) \text{ at } |\Omega\tau - \phi| \leqq \frac{\pi}{2} \\ 0 \text{ at } \frac{\pi}{2} \leqq (\Omega\tau - \phi) \leqq \frac{3\pi}{2}. \end{cases}$$

In the first approximation, the structure of the soil and its thermophysical properties, λ, c_s, $\rho \neq f(y)$, being assumed constant, one can show that the soil temperature, $T_{y=0}$, on the surface is uniquely determined by the complex

$$\gamma = (\lambda c_s \rho)^{-1/2}. \qquad (2)$$

Here, the soil heat capacity c_s and density ρ are governed by the chemical nature of the minerals of which the surface is formed, but they depend non-uniquely on its structure. The effective thermal conductivity λ of the layer can be a strong function of both the pattern of the soil structure (the presence of nonconnecting or interconnection pores, their mean size, degree of consolidation of soil particles) and the type of the component filling the pores under the existing ambient conditions (gas pressure and temperature).

METHOD OF FORECAST

The forecast of the planetary surface structure can be shown by an example of Moon investigation. The first lunar surface characteristics have been secured in the visible wavelength spectrum with the aid of the Earth-based optical methods. By comparing the albedo (reflectivity), colour, scattering indicatrix of the solar radiation and its polarization for different model structures (solid, porous or crushed rocks and soils of the Earth; metal surfaces, grasses, lichens, mosses, artificial interlacing of fibres and wires, etc. [1]), it has been possible to find that a thin upper layer (several millimeters deep) is composed of porous material similar to finely granulated tuff, dust of 10×10^{-6} - 10×10^{-3} m grains or moss-like structure.

The optical observations of the visible spectrum failed to provide data on the structure of a more deep-seated layer. The Soviet ("Luna-1,2" and "Zond-3") and American ("Ranger" and "Lunar Orbiter") spacecraft photographs of the Moon have not made any essential specifications to the nature of the soil structure. As Gold has put it, pictures taken from the spacecrafts are like a "magic mirror" in which each scientist sees the reflection of his own theory of the Moon origin and of its surface properties [3]. Really, the hypotheses about the lunar soil embrace a wide range of structures from dust "maria", hundreds of meters deep, to consolidated rocks.

A considerable progress in exploration of the lunar soil has been achieved when carrying out the studies of the proper and reflected (location) r.f. radiation in the wavelength range from millimeters to a meter and a

Table 1. Comparison of the forecast data and measurements of different lunar soil properties

Soil properties	Initial data and forecast results				"Luna"-program, 1966–1973, U.S.S.R.		"Surveyor"-program, 1966–1968, U.S.A.		"Apollo"-program, 1969–1972, U.S.A.	
1	2		3		4		5		6	
Mineralogical composition	Basalt				Basalt		Low iron-content basalt		Basalt, andesito-basalt, plagioclase, pyroxene	
in %	O	62±4	SiO_2	57±3	SiO_2	44.4	O	58±5	SiO_2	41
	Si	20±1	Al_2O_3	16±1	TiO_2	0.56	Si	18±4	CaO	10.5
	Al	7±0.5	Fe_2O_3	1±2	Al_2O_3	22.9	Al	9±3	MgO	8
	Mg	2±1	FeO	5±1	FeO	7.03	Mg	4±3	FeO	18
	Fe	2±0.5	CaO	5.5±2.5	MgO	9.7	Fe	2±1	Al_2O_3	11.3
	Ca	2±1	MgO	3.5±2	CaO	18.2	Ca	6±1	Na_2O	0.6
	K	1.5±0.5	Na_2O	4±0.5	Na_2O	0.55	Na	3	K_2O	0.2
	Na	1.5±0.5	K_2O	3±1	K_2O	0.1			TiO_2	10
			TiO_2	1±0.5						
Mean size of soil particles	$(5 \times 10^{-2}–1)$mm						$(2.10^{-3}–60.10^{-3})$mm		$(0.2–83) \times 10^{-3}$ mm $(50–150) \times 10^{-3}$ mm	
Soil density	(1.2–1.8)g/cm^3				1.52 g/cm^3		(1.0–1.5)g/cm^3		(1.1–1.8)g/cm^3 1.8–1.9 g/cm^3	
Density of particles	2.6 g/cm^3						(3.2–2.8)g/cm^3		(2.9–3.2)g/cm^3	
Depth of test layer	Up to 2 m				35 cm		(8–17.5)cm		Up to 4 m	
Thermal conductivity of rock grains	(2 3)W/mK									
Heat capacity	840 J/kgK									
Effective thermal conductivity of soil	(0.018–0.006)W/mK									
Character of soil structure	granular, loosely bound				granular, loosely bound		fine-grained, loosely bound with admixture of gravel and large stones		slightly bound granular soil	

half. Measurements of the loss tangent and of the dielectric constant made it possible to determine the chemical composition and the density of the soil to the depth of several meters (Table 1). Proceeding from the assumption that the minerals of the lunar surface are similar to the terrestrial soils, we can take for them, with some reservation, the heat capacities of terrestrial soils whose difference did not exceed 10% at normal conditions.

At the same time, the effective thermal conductivity, λ, of terrestrial soils under lunar-like conditions (gas pressure below 1×10^2 N/m^2) could vary by three orders, ranging from $(1–5) \times 10^{-3}$ W/mK for dusty soil to (2–3) W/mK for dense sedimentary or igneous rocks.

This essential difference in thermal conductivities of possible soil patterns made it difficult to choose appropriate analogs by an experimental approach alone. It was thought worthwhile therefore to resort also to the analytical means of determining the effective thermal conductivity of porous bodies. Having calculated the effective thermal conductivities of different porous models and substituting them into the RHS of relation (2) together with the known (or assumed) values of heat capacity c_s and density ρ, one can estimate the complex γ_{calc} which is then compared with γ_{exp} obtained by radio-astronomical observations.

The postulated type of the planetary surface structure is chosen when these both values, γ_{calc} and γ_{exp}, coincide (Fig. 2). Besides, the forecast of the lunar surface structure should provide for the possibility of diffusive sintering of soil particles under high vacuum at temperature oscillations between 120 and 450 K [1]. It is, therefore, reasonable to consider two extreme models of soil structure—unconsolidated beds and solid porous body. These models are to be complied with the minimum and maximum values of the complex γ_{calc}.

If the measured values of γ_{exp} lie between the possible extremes, further specification of the surface soil structure parameters is being made [4]. For the sake of unification, calculation of the complex γ is reasonable to be performed using a more general

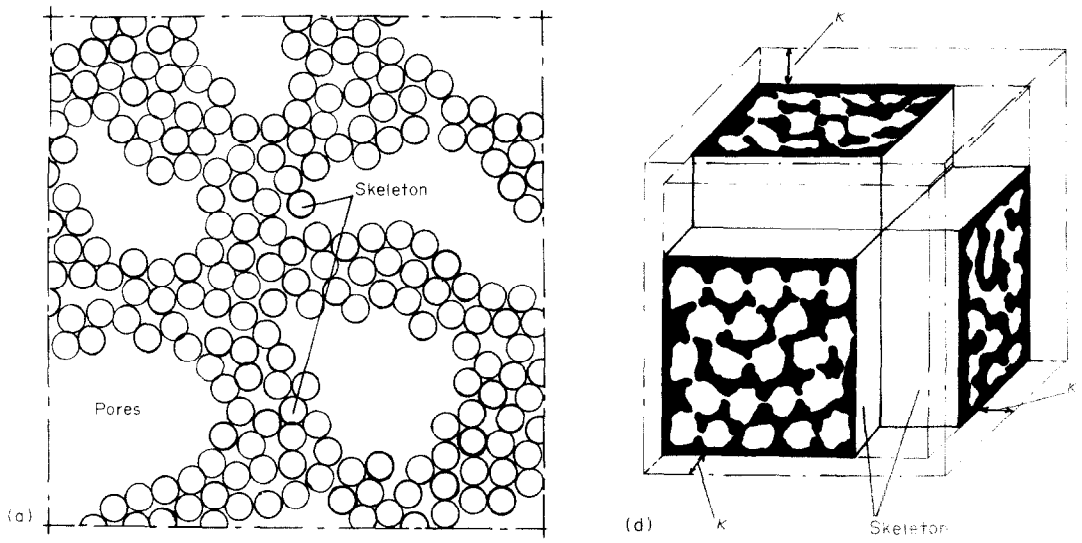

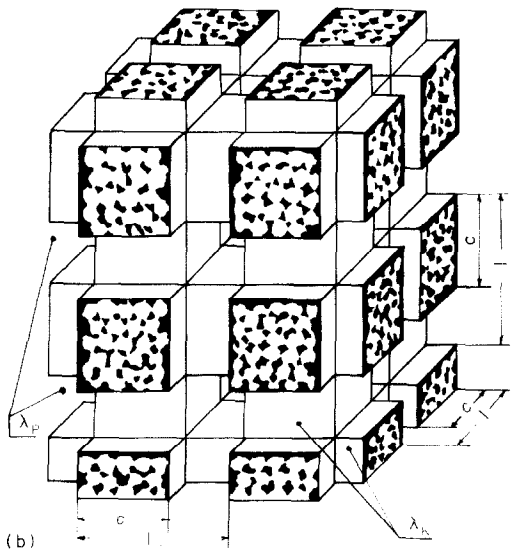

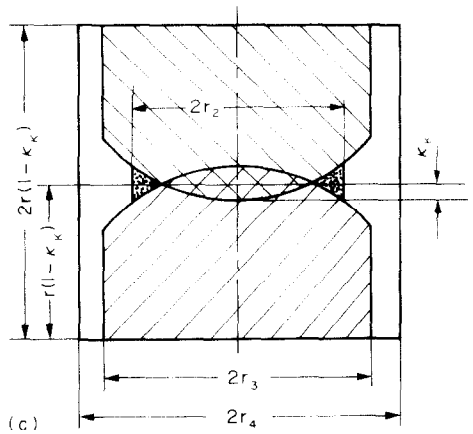

FIG. 1. Generalized model of porous granular soil structures: (a) schematic two-dimensional drawing of chaotic structure of real soil; (b) partially ordered space model of soil structure; (c, d) elementary cells of the second-order structure (a frame pierced with larger cavities).

model of partly consolidated (sintered, cemented) granular soil ("consolidated beds") embracing the whole possible range of the complex γ_{calc} [5, 7]. The above extremes are particular cases of the generalized model.

The structure of the bound granular material is schematically presneted in Figs. 1(a) and (b). The structure is seen to have a "frame" (skeleton) formed with chaotic but relatively dense arrangement of grains. The grains may slightly contact with one another at contact points (loosely-strewed granular systems) or have a very large contact spot (dense consolidated materials). The frame itself ("the first-order structure") is pierced with a spatial network of larger empties which, coupled with the frame [5, 7], form the "second-order structure". The degree of sintering (cohesion) of the soil may be characterized by the radius, r_2, of the real contact spot of the grains, of which the frame is formed (Fig. 1(c)).

THERMAL CONDUCTIVITY OF SOIL MODEL

It has been shown above that the main complexity in calculating the complex γ_{calc} is introduced by estimation of the effective thermal conductivity, λ, of the chosen model. Theoretical justification for the method of calculation of λ for the model presented in Fig. 1 has been given elsewhere [5, 7], therefore, we shall only summarize here the basic formulas furnishing them with some comments.

First we shall specify the main geometrical parameters to describe the frame of the model chosen. An essential part will be played further by the coordination number N, which is the number of contacts per one particle. Reference [5] suggests the following relationship for N, which depends on the porosity of the frame m_{2k}^0, for unconsolidated material

$$N = \frac{3 + m_{2k}^0 + [(m_{2k}^0)^2 - 10m_{2k}^0 + 9]^{1/2}}{2m_{2k}^0}. \quad (3)$$

and it is assumed that N does not vary with consolidation of the system.

Consider now the geometrical parameters to describe the first-order structure, i.e. the frame. As is shown in [5, 7], the effective thermal conductivity of the frame (Fig. 1b) is consistent with that of some averaged cylindrical element (Fig. 1c), which is governed by several geometrical parameters: grain radius r, contact-spot radius r_2, radius r_3 of a solid portion of the cylindrical element and r_4 of the circular pore. Also, with consolidation of particles (as a result of compression, sintering, etc.) there appears linear deformation, κ_k, of a particle (Fig. 1c) whose value depends unambiguously on porosity m_{2k}^0, porosity m_2^0 for unconsolidated beds and on porosity m_2 of the same material upon consolidation

$$\kappa_k = \left[1-\left(\frac{1-m_2^0}{1-m_2}\right)^{1/3}\right]\frac{1-(1-m_{2k}^0)^{1/3}}{1-(1-m_2^0)^{1/3}}. \quad (4)$$

It can be shown that the relative values of $y_i = r_i/r$ $(i=2,3,4)$ are synonymously related with the parameters N, m_{2k}^0 and κ_k by the following expressions [5]:

$$y_2 \simeq 1.7\times10^{-4}(\rho)^{1/2}+\frac{2}{N}\left[\frac{\kappa_k(N-1)}{1-(1-m_{2k}^0)^{1/3}}\right]^{1/2};$$
$$y_3 = \frac{2(N-1)^{1/2}}{N}, \quad y_4 = y_3\frac{1-\kappa_k}{(1-m_{2k}^0)^{1/3}}, \quad (5)$$
$$\times[\rho] = \mathrm{kg/m^3}.$$

Consider now the geometrical parameters of the second-order structure, or putting it another way, of the whole model under study.

The thermal conductivity, λ, of the soil structure is calculated by the formula, the arguments for which are given in [5]

$$\lambda = \lambda_k\left[c^2+v(1-c)^2+\frac{2vc(1-c)}{vc+1-c}\right], \quad (8)$$

where an intermediate parameter c is uniquely related with the porosity by the equation

$$m_{22} = 2c^3-3c^2+1,$$

whose analysis is made in [5].

The parameter v is related with the thermal conductivity, λ_k, of the frame, radiative λ_r and molecular λ_m components of the thermal conductivity of the whole system by the equation

$$v = \frac{\lambda_r+\lambda_m}{\lambda_k}.$$

We may show [5, 7] that λ_r and λ_m can be calculated within a sufficient accuracy by

$$\lambda_r = 0.3\left(\frac{T}{100}\right)^3\frac{1}{\alpha}, \quad \alpha = \frac{(2-\varepsilon)c^2(2-c)}{1.5d(1-\kappa)},$$
$$\lambda_m = \frac{\lambda_g}{1+\dfrac{B}{H\delta_2}}, \quad (9)$$
$$\delta_2 = 3d\frac{1-\kappa}{1/c-1}.$$

So, by now the undetermined value is the effective thermal conductivity λ_k of the frame. For the consolidated system, it can be estimated by the formula [5, 7]

$$\frac{\lambda_k}{\lambda_1}y_4^2 = \frac{y_2^2}{\Phi}+\frac{1-\kappa_k}{\dfrac{D}{y_3^2-y_2^2}+\dfrac{1-v_1}{2v_1\left[D-F+W\ln\left(1+\dfrac{F-D}{W-F}\right)\right]}}+v_2(y_4^2-y_3^2),$$

$$F = (1-y_2^2)^{1/2}, \quad D = (1-y_3^2)^{1/2}, \quad W = \frac{\dfrac{B}{Hd}+1-\kappa_k-v_1(1-y_3^2)^{1/2}}{1-v_1}, \quad (10)$$

$$\Phi = v_1^2(7.5-11v_1+4.5v_1^2)\left(1-\frac{y_2}{y_3}\right)+\frac{y_2}{y_3}.$$

The overall porosity, m_2, of the consolidated system, initial porosity, m_2^0, and relative total deformation of the system are related as (Fig. 1d)

$$\kappa = 1-\left(\frac{1-m_2^0}{1-m_2}\right)^{1/3}. \quad (6)$$

Another geometrical parameter, which is the porosity of the second-order structure with open pores, is of the form

$$m_{22} = 1-\frac{1-m_2^0}{1-m_{2k}^0}\left(\frac{1-\kappa_k}{1-\kappa}\right)^3. \quad (7)$$

In formulas (10), the physical parameters v_i are of the form

$$v_1 = \frac{\lambda_{r1}+\lambda_g}{\lambda_1}, \quad v_2 = \frac{\lambda_{r2}+\lambda_{m2}}{\lambda_1},$$

where

$$\lambda_{r1} = 2.3\times10^{-7}T^3\varepsilon\frac{\delta_1}{2-\varepsilon}, \quad \delta_1 = \frac{d}{N}(1-\kappa_k),$$
$$\lambda_{r2} = 0.3d(1-\kappa_k)\left(\frac{T}{100}\right)^3,$$
$$\lambda_{m2} = \lambda_g\left[1+\frac{B}{Hd(1-\kappa_k)}\right],$$
$$B = \frac{4\times10^5\Lambda(c_p/c_v)(2-a)}{[1+(c_p/c_v)]aPr}.$$

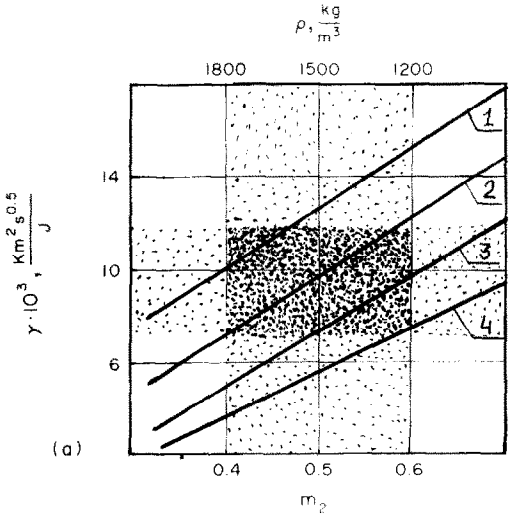
ρ, kg/m³
1800
1500
1200
γ·10³, Km²s^0.5/J
14
10
6
1
2
3
4
(a)
0.4
0.5
0.6
m₂

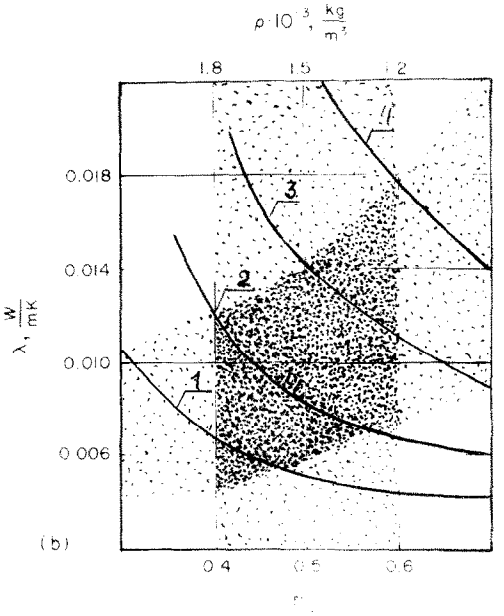
ρ·10⁻³, kg/m³
1.8
1.5
1.2
λ, W/mK
0.018
0.014
0.010
0.006
1
2
3
(b)
0.4
0.5
0.6

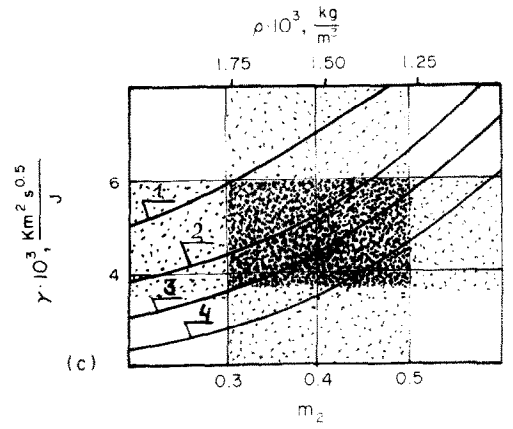
ρ·10⁻³, kg/m³
1.75
1.50
1.25
γ·10³, Km²s^0.5/J
6
4
1
2
3
4
(c)
0.3
0.4
0.5
m₂

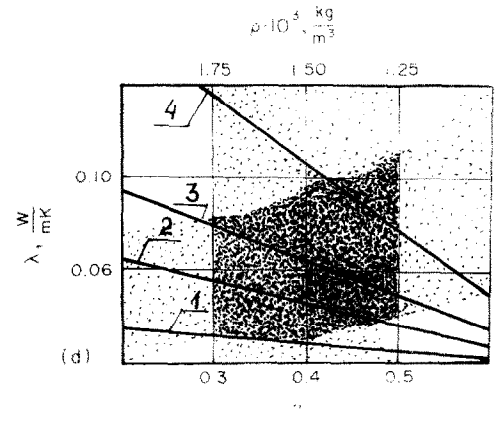
ρ·10⁻³, kg/m³
1.75
1.50
1.25
λ, W/mK
0.10
0.06
4
3
2
1
(d)
0.3
0.4
0.5

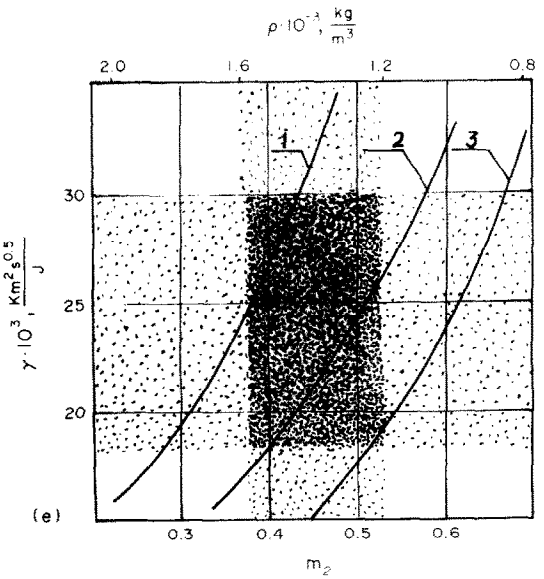
ρ·10⁻³, kg/m³
2.0
1.6
1.2
0.8
γ·10³, Km²s^0.5/J
30
25
20
1
2
3
(e)
0.3
0.4
0.5
0.6
m₂

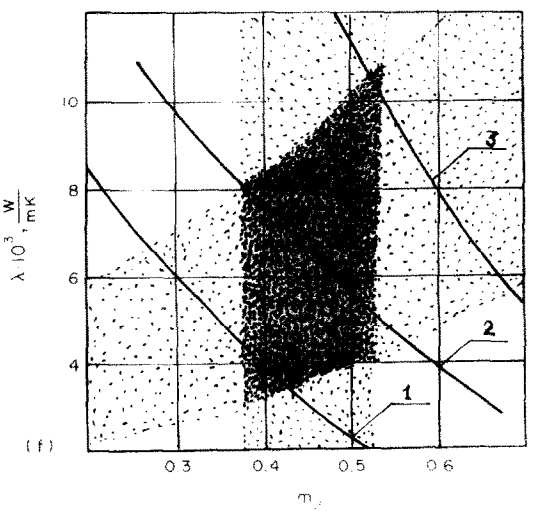
λ·10³, W/mK
10
8
6
4
1
2
3
(f)
0.3
0.4
0.5
0.6

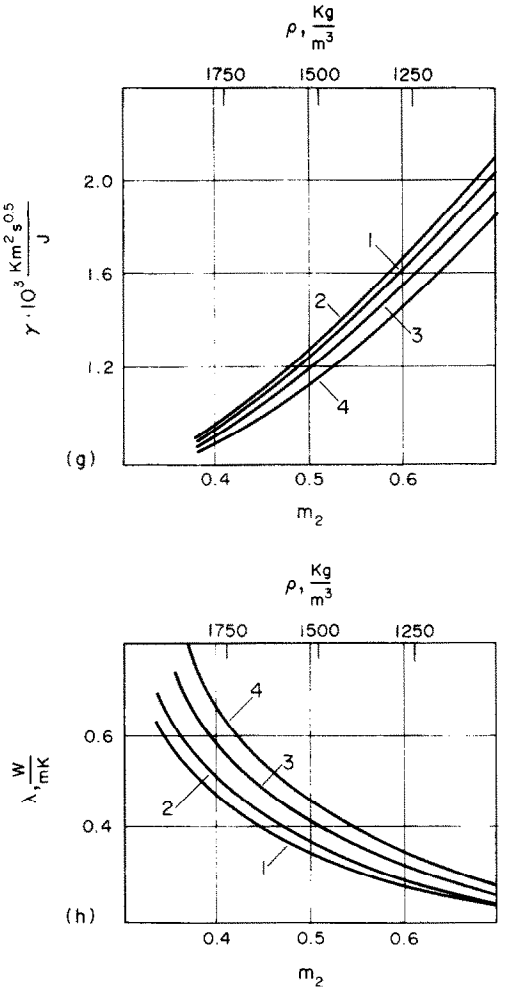

FIG. 2. Comparison of calculated and measured values of the complex γ (a,c,e,g) and thermal conductivity (b,d,f,h) for the soils with different degree of consolidation: —, calculated values; : : :, scattering of supposed values of soil porosity and measured values of the complex γ; (a,b) calculations for Moon conditions: $T = 300$ K, $H = 1 \times 10^{-5}$ mmHg, $d = 0.1 \times 10^{-3}$ m, $\lambda_1 = 2$ W/mK; 1. $y_2 = 3 \times 10^{-3}$; 2. $y_2 = 5 \times 10^{-3}$; 3. $y_2 = 1 \times 10^{-2}$; 4. $y = 2 \times 10^{-2}$; (c,d) calculations for Mars conditions: $T = 200$ K, $H = 5$ mmHg, $d = 0.1 \times 10^{-3}$ m, $\lambda_1 = 2$ W/mK, CO_2 atmosphere; 1. $y_2 = 2 \times 10^{-3}$; 2. $y_2 = 1 \times 10^{-2}$; 3. $y_2 = 2 \times 10^{-2}$; 4. $y_2 = 4 \times 10^{-2}$; (e,f) calculations for Mercury conditions: $T = 100$ K, $H = 1 \times 10^{-5}$ mmHg, $d = 0.1 \times 10^{-3}$ m, $\lambda_1 = 2$ W/mK; 1. $y_2 = 2 \times 10^{-3}$; 2. $y_2 = 5 \times 10^{-3}$; 3. $y_2 = 1 \times 10^{-2}$; (g,h) calculations for Venus conditions: $T = 773$ K, $H = 100$ atm, $d = 0.1 \times 10^{-3}$ m, $\lambda_1 = 2$ W/mK, CO_2 atmosphere; 1. $y_2 = 5 \times 10^{-3}$; 2. $y_2 = 2 \times 10^{-2}$; 3. $y_2 = 5 \times 10^{-2}$; 4. $y_2 = 1 \times 10^{-1}$.

The initial data for the analysis performed are as follows. For γ_{calc} to be calculated, the knowledge of c_s, ρ and λ of the soil is necessary. In its turn, the thermal conductivity, λ, of the soil depends on the mean diameter of particles d; emissivity of particles ε at mean temperature T; thermal conductivity, λ_1, of grains (with zero porosity); gas-filler pressure H; Prandtl number Pr; isobaric-to-isochoric heat-capacity ratio for gas c_p/c_v; mean free molecular path length Λ for gas-filler at normal pressure; coefficient, a, of gas molecule accommodation to grain material; thermal conductivity of gas filler λ_g which is equal to the sum of radiant λ_r and molecular λ_m conductivities; initial m_2^0 and final m_2 porosities of the soil.

COMPARISON OF THEORETICAL AND OBSERVED VALUES

The above scheme of deriving the soil thermophysical parameters has been first used to forecast the structure of the lunar surface [4]. The results obtained are as follows.

Moon

The set of initial data for calculation, thermophysical properties of the lunar soil and its structural characteristics are given in Table 1 and Figs. 2(a) and (b). It is usual for radio-astronomical results to scatter by $\pm 25\%$ (from the mean value). Similar scatter is typical of the data on the surface soil density. In the coordinate systems $\gamma = f(\rho)$ and $\gamma = f(m_2)$ the measured results form a rectangular region (Fig. 2a).

The values of γ_{calc} are plotted in Figs. 2(a) and (b) as curves whose set is consistent with the theory of combination of possible values in a wide range of the governing parameters $(y_2, m_2, d, \lambda_1, \ldots)$. The mean values of the temperature T entering the design equations correspond to average-volume temperatures of the layers of any thickness in radio-astronomical observations.

In order to take into account the effect of differences in the thermal conductivities, λ_1, of the grains, the calculations were performed for $\lambda_1 = 2$ W/mK and $\lambda_1 = 3.5$ W/mK, these values covering the range of thermal conductivities of the most widely spread terrestrial soils and their lunar analogs.

This structure-forecasting method provided good results when the lunar surface was studied [1, 4] with the aim of designing soft-landing systems. It seems to be likewise perspective in forecasting the soil structure on Mars, Mercury and Venus.

Mars

As seen from Figs. 2c and d, the scatter (dashed area) of the measured values of γ_{exp} for Mars is characteristic of the materials with different porosity m_2 (density ρ) and varying relative radius y_2 of the contact spot of particles.

If we assume for the density of the Martian surface $1300 \leqq \rho \leqq 1800$ kg/m^3 [6], which corresponds to porosity $0.3 \leqq m_2 \leqq 0.5$ (at $\rho_0 \simeq 2600$ kg/m^3), then it can be easily seen that complexes γ_{calc} and γ_{exp} agree for small contact spots, $2 \times 10^{-3} \leqq y_2 \leqq 5 \times 10^{-2}$, characteristic of loosely bound materials (as a rule, for terrestrial dry sand $y_2 \simeq (1\text{–}3) \times 10^{-3}$). The assumed thermal conductivity of the Martian soil is apparently in the range $0.03 \leqq \lambda \leqq 0.11$ W/mK.

Mercury

Similar calculations and measurements for Mercury yield appreciably lower values for soil thermal conductivity because of low residual atmospheric pressure $H = 1 \times 10^{-4}$ mm Hg (Figs. 2f and g) and correspondingly, higher values of γ.

At higher temperatures, more essential sintering of soil particles with the relative radius of the sintering spot $3 \times 10^{-3} \leqq \gamma_2 \leqq 1 \times 10^{-2}$ may be expected on the Mercury surface.

Venus

In Figs. 2(i) and (k), the γ_{calc} are plotted for the conditions on Venus (in the CO_2 atmosphere at $H = 100$ atm, temperature $T = 773$ K and density $1200 \leqq \rho \leqq 2600$ kg/m^3). When obtained, the data on the temperature field in the Venus surface may be used to estimate the range of possible γ-values and to determine the soil characteristics.

REFERENCES

1. V. S. Troitsky and T. V. Tikhonova, Thermal radiation of Moon and physical properties of its upper layer. *Izv. VUZov. Radiofiz.* **13**(9), 1273–1311 (1970).
2. V. D. Krotikov and O. B. Shchuko, On the changes of Martian integral radio emission between oppositions. *Izv. VUZov. Radiofiz.* **16**(12), 1811–1815 (1971).
3. I. I. Cherkasov and V. V. Shvarev, *Lunar Soil*. Nauka, Moscow (1975).
4. G. N. Dulnev, Yu. P. Zarichnyak and B. L. Muratova, On possible structure of lunar surface. *Izv. VUZov. Radiofiz.* **9**(5), 849–857 (1965).
5. G. N. Dulnev and Yu. P. Zarichnyak, *Thermal Conductivity of Mixtures and Composite Materials*. Energiya, Moscow (1974).
6. A. E. Basharinov, Yu. P. Vetukhnovskaya, V. N. Galaktionov, I. B. Drozdovskaya, S. T. Egorov, M. A. Kolosov, V. D. Krotikov, N. N. Krupenko, A. D. Kuz'min, V. A. Lodygin, L. I. Maladyaeve, E. P. Omel'chenko, V. S. Troitsky, N. Ya. Shapirovskaya, A. M. Shchutko and O. B. Shchuko, The results of observation of Martian radio emission based on the experimental evidence on the AMS "Mars-3", *Kosm. Issled.* **11**(5), 803–806 (1973).
7. G. N. Dulnev, Yu. P. Zarichnyak and M. A. Eremeyev, Thermal conductivity of bound materials. *Inzh.-Fiz. Zh.* **27**(1), 55–62 (1974).

ESTIMATION DE LA STRUCTURE DE LA SURFACE DE LA LUNE, DE MARS, DE MERCURE ET DE VENUS, A PARTIR DES OBSERVATIONS RADIO-ASTRONOMIQUES SUR LEURS CONDITIONS THERMIQUES

Résumé—Les derniers progrés dans la théorie du transfert de chaleur dans les systèmes hétérogènes par la modélisation des structures complexes, rendent possibles à partir de l'analyse des observations radiophysiques des conditions thermiques des planètes, la résolution du problème inverse, à savoir la détermination de la texture du sol des planètes à partir de leurs propriétés thermophysiques. La méthode utilisée en couplage avec les propriétés électro-physiques et optiques (constante diélectrique et perméabilité magnétique, atténuation et polarisation du rayonnement permet d'estimer la structure du sol des planètes les plus proches de la terre, la lune, Mars, Mercure et Vénus.

VORHERSAGE DER OBERFLÄCHENBESCHAFFENHEIT VON MOND, MARS, MERKUR UND VENUS AUF DER GRUNDLAGE RADIO-ASTRONOMISCHER BEOBACHTUNGEN IHRER THERMISCHEN VERHÄLTNISSE

Zusammenfassung—Die jüngsten Fortschritte der Theorie des Wärmetransports in heterogenen Systemen, d.h. die mathematische Modellierung komplexer Strukturen, machen es möglich, durch Auswertung von radiophysikalischen Präzisionsbeobachtungen der thermischen Verhältnisse auf den Planeten das inverse Problem zu lösen, nämlich die Bodenstruktur der Planeten aus ihren thermophysikalischen Eigenschaften zu bestimmen. Die beschriebene Methode zusammen mit der Fernmessung elektro-physikalischer und optischer Eigenschaften (Dielektrizitätskonstante und magnetische Permeabilität, Abschwächung und Polarisation der Strahlung) gestattet Voraussagen über die Bodenstruktur der nächsten Nachbarn der Erde im Sonnensystem – Mond, Mars, Merkur und Venus.

ПРОГНОЗИРОВАНИЕ СТРУКТУРЫ ГРУНТА В ПОВЕРХНОСТНОМ СЛОЕ ЛУНЫ, МАРСА, МЕРКУРИЯ И ВЕНЕРЫ ПО РЕЗУЛЬТАТАМ РАДИОАСТРОНОМИЧЕСКИХ ИЗМЕРЕНИЙ ИХ ТЕПЛОВЫХ РЕЖИМОВ

Аннотация — Использование современных достижений теории теплопереноса в гетерогенных системах (моделирование сложных структур и приближенное математическое описание их свойств) на основе анализа результатов прецизионных радиофизических измерений теплового режима поверхностного покрова планет позволяет решить обратную задачу — определение структуры грунта планет по их теплофизическим характеристикам.

Предлагаемый метод в сочетании с дистанционными методами изучения электрофизических и оптических свойств (диэлектрической и магнитной проницаемости, затухания и поляризации излучения) создает возможность прогнозирования строения грунта ближайших к Земле планет солнечной системы — Луны, Марса, Меркурия и Венеры.